JOURNAL OF PROPULSION AND POWER
Vol. 20, No. 1, January–February 2004

Ultrasonic Measurement of the Pressure-Coupled Response Function for Composite Solid Propellants

Thomas J. Hafenrichter,* Jeffrey J. Murphy,† and Herman Krier‡
University of Illinois at Urbana—Champaign, Urbana, Illinois 61801

Transient phenomena associated with solid-propellant combustion are examined by means of an oscillatory burner designed to create pressure oscillations through the use of a rotary nozzle. The oscillatory burner is designed to operate at pressures up to 20.7 MPa (3000 psi), with the target operating pressure achieved through prepressurization with an inert gas (helium) and manipulation of constant and variable-area nozzle diameters. A spherically focused 1-MHz ultrasound transducer is pulsed at 2.5 kHz through the bottom of the propellant to obtain the thickness–time profile of the propellant, which is then converted to a burning rate by taking the time derivative. Two piezoelectric pressure transducers simultaneously record the pressure–time history of each experiment. The burning rate and pressure are then used to calculate the pressure-coupled response of each test. The experiments presented here were motivated by three primary goals. The first was to investigate the effect of propellant composition on the response function. The second was to evaluate effect of mean pressure on the response of propellants, and the third was to investigate the response of a propellant within a plateau region. These experiments targeted mean pressures of 2.0, 5.0, and 12.5 MPa at frequencies ranging from 20–200 Hz.

Nomenclature

a = prefactor in burning rate law
c = speed of sound
f = frequency, Hz
G = spectral density function
i = $(-1)^{\frac{1}{2}}$
n = burning-rate law pressure exponent
p = pressure
R = response function
$\Re$ = cross-correlation function
$\dot{r}$ = burning rate
t = time
x = distance or arbitrary function
y = arbitrary function
α = thermal diffusivity
Δ = change
δ = round-trip time
τ = time delay
Φ = phase of response function
Ω = nondimensional frequency, $2\pi f\alpha/\bar{r}^2$
ω = angular frequency

Subscripts

eff = effective
f = final or flame
0 = reference value

Superscripts

- = steady-state or mean quantity
′ = unsteady quantity
. = time derivative

Introduction

THE primary focus of this work is to obtain the pressure-coupled burning-rate response of several composite solid propellants at different frequencies and pressures. These results are used to determine the effect of propellant composition and mean pressure on this response, as well as evaluate the response of a propellant at pressures within a plateau region.

The burning-rate and response function data presented here are obtained using an ultrasound measurement technique previously developed at the University of Illinois.[1,2] This method differs from earlier ultrasound techniques in that digital-signal-processing technology is utilized to analyze the ultrasound pulse-echo data. Digital techniques provide superior signal detection and are far more flexible than analog techniques.

Currently, the industry standard for transient measurements is the T-burner; however, this technique is generally limited to frequencies ranging from 300–4000 Hz and requires limiting assumptions to simplify the theoretical acoustic analysis.[3,4] The ultrasound measurement system discussed here directly measures the burning surface location, which does not incorporate any simplifying linearization. Burning-rate data are obtained directly from the ultrasound thickness calculations synchronized with the pressure–time history. In addition, ultrasound is suitable for measurements in the low-frequency range (<300 Hz). Therefore, the technique serves as a supplement to the high frequency T-burner data.

The steady-state burning-rate curve of a solid propellant is a function of pressure and is typically fit to an equation of the form:

$$\dot{r} = ap^n \tag{1}$$

which is known as Vieille's or St. Robert's burning-rate law, where a is a dimensional empirical constant and the pressure exponent n is given by $(\partial \ln \dot{r}/\partial \ln p)_{T_0}$.

From Eq. (1) it is evident that the propellant burning rate and chamber pressure are uniquely interdependent. Therefore, a proper tool for predicting motor instability will relate these two quantities. Moreover, because instabilities can only be driven when the burning rate and pressure have the proper phase relationship, this must be taken into account in the response calculation. The pressure-coupled

Received 18 June 2002; revision received 1 August 2003; accepted for publication 5 August 2003.

*Predoctoral Fellow, Department of Mechanical and Industrial Engineering, 1206 West Green Street; currently Senior Member of Technical Staff, Sandia National Laboratories, P.O. Box 5800, MS1452, Albuquerque, New Mexico 87185. Member AIAA.

†Graduate Research Assistant, Department of Mechanical and Industrial Engineering, 1206 West Green Street; currently Postdoctoral, Sandia National Laboratories, P.O. Box 969, MS9052, Livermore, CA 94551. Member AIAA.

‡Richard W. Kritzer Distinguished Professor, Department of Mechanical and Industrial Engineering, 1206 West Green Street. Fellow AIAA.

burning-rate response is defined by the following equation:

$$R_{\dot{r},p} = \frac{\dot{r}'/\bar{\dot{r}}}{p'/\bar{p}} \tag{2}$$

Thus, the response function represents the dynamic pressure-burning relationship for a specific propellant. The normalized pressure and burning rate for a 50-Hz test of Alliant #5—an unaluminized composite propellant—at 2.07 MPa is shown in Fig. 1. Note that the pressure and burning rate are out of phase (represented by Φ).

The expression in Eq. (1) can be represented in the frequency domain by the following equation:

$$R_{\dot{r},p} = (\bar{\dot{r}}/\bar{p})(G_{\dot{r}}/G_p) \tag{3}$$

where $G_{\dot{r}}$ and G_p represent the Fourier transforms of the burning rate and pressure, respectively.[2] Because the response is calculated in the frequency domain, it can have both real and imaginary components. The real part of the response is the component that is in phase with the pressure and can, therefore, couple with pressure oscillations to drive instabilities. The imaginary part represents the out-of-phase component. Alternatively, the response can be expressed as a magnitude and phase angle. A geometric depiction of the response function is presented in Fig. 2. For a true steady-state condition the linearized form of the burning-rate law [Eq. (1)] is $(\dot{r}'/\bar{\dot{r}}) = n(p'/\bar{p})$, so that the response function given in Eq. (3) must approach n at low frequencies.

The response of a propellant at a particular pressure and frequency condition can lie within any of the four quadrants shown in Fig. 2. However, the response can only have a positive real part when the phase is between −90 deg and +90 deg. This is a critical observation because the more positive the real part of the response, the more potential the propellant has to couple with the pressure to drive

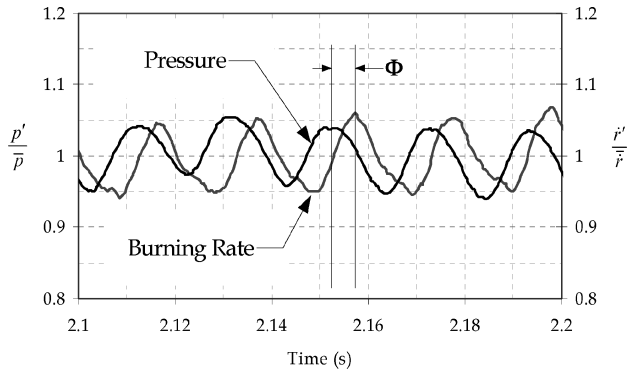

Fig. 1 Normalized pressure and burning-rate curves taken from a 50-Hz test of Alliant #5 at 2.07 MPa.

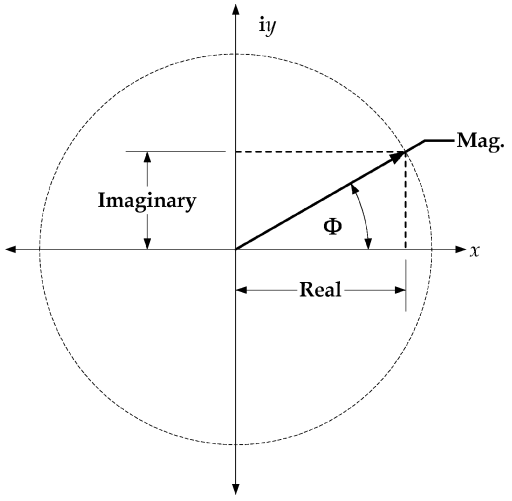

Fig. 2 Geometric representation of the pressure-coupled response function.

instabilities. Therefore, propellants that burn in phase with pressure oscillations are generally more problematic.

Overview of Experimental Method

Generally, thickness measurements are made using ultrasound echolocation by sending a pulse into the sample by means of an ultrasound transducer coupled to the propellant surface. The pulse is reflected from the burning surface after it travels through the propellant. The reflected pulse then returns to the transducer, and the time it takes for the pulse to complete the round trip is recorded. The sample thickness is subsequently determined by the formula:

$$\Delta x = c\Delta t/2 \tag{4}$$

where Δx is the thickness and Δt is the measured round-trip time. The material speed of sound c is typically determined from previous measurements using samples of known length.[1]

Burning-rate measurements of solid propellants utilize this same concept. Thickness measurements are taken repeatedly throughout an experiment, and the derivative of these measurements with respect to time gives the burning rate of the propellant. Through manipulation of transducer properties, such as the pulse frequency and the sample frequency (measurements per second), an accurate measure of the burning rate can be attained. These measurements, however, are complicated because propellant is not an acoustically simple solid. Composite propellants, as those tested in this study, are nonlinear viscoelastic materials. A burning propellant has a "rough" surface, which, because of the oxidizer particle size variation, can be covered with melting binder and/or aluminum. In addition, the large temperature gradient in the thermal layer near the burning surface affects the propellant density, speed of sound, and acoustic impedance.[5] The chamber pressure further complicates these issues by compressing the propellant, thereby changing both the thickness and speed of sound. The use of sophisticated techniques to detect the echo as well as applying a pressure correction can help resolve some of these issues.

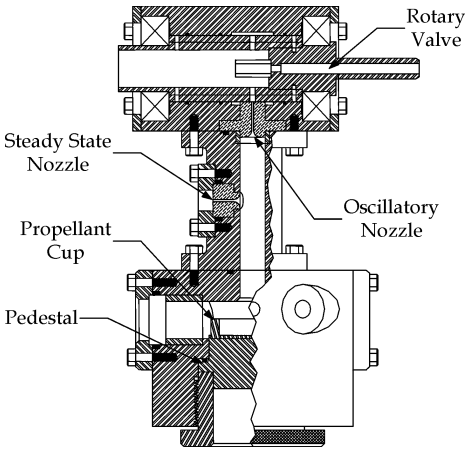

Fig. 3a Schematic of the oscillatory burner.

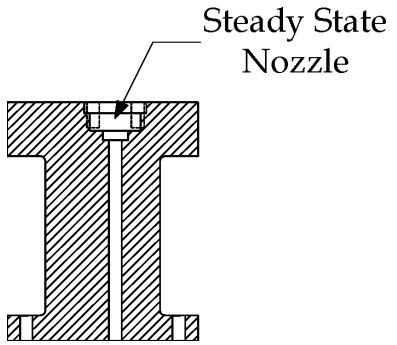

Fig. 3b Steady-state chamber throat.

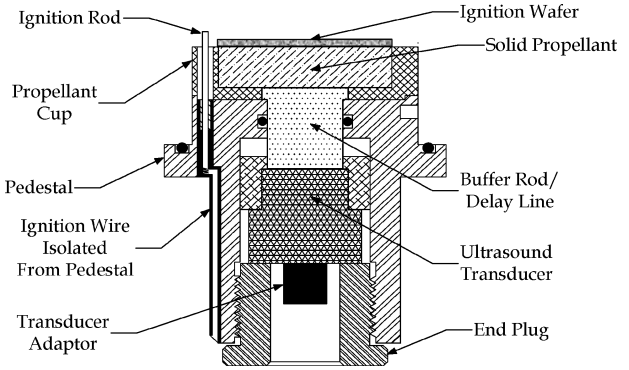

Fig. 4 Pedestal assembly housing the ultrasound transducer and propellant sample.

Experimental Apparatus

A schematic of the oscillatory combustion chamber developed and tested at the University of Illinois at Urbana—Champaign is given in Fig. 3a (Refs. 2, 6–8). The rotating valve design is based upon a very similar system developed at United Technologies Chemical Systems Division (CSD).[9] The average chamber pressure is enhanced and controlled by helium-gas prepressurization and proper selection of both the constant and variable-area nozzle diameters. The chamber is designed to operate at pressures up to 20 MPa (3000 psi) with a factor of safety of 5. Two PCB Piezotronics helium-bleed piezoelectric pressure transducers record the pressure trace for each experiment. These transducers have a response time of 20 μs.

The propellant samples are approximately 32×32 mm (1.25×1.25in.), with a height ranging from 7–11 mm. The samples are cut to uniform thickness to ensure a constant endburning surface area. To achieve uniform ignition, an electric current is passed through a Nichrome wire that is secured between the test sample and a thin propellant wafer [a hand-mixed ammonium perchlorate/hydroxyl-terminated polybutadiene (AP/HTPB) propellant], thereby igniting the wafer, which immediately ignites the test sample. Side burning of the propellant sample is avoided through an inhibitor (RTV sealant) applied to the edges of the propellant. The inhibitor also serves to prevent the sample from dislodging from the propellant cup during a test.

A belt driven 2-hp variable speed motor operates the rotary valve, which has 20 holes drilled about its circumference. The maximum oscillation frequency of the system is 600 Hz based upon the current motor and pulley configuration. The motor control box is equipped with a dial to properly set the motor speed. An light-emitting diode (LED) display is connected to the motor control box, and the reading of the display is calibrated by a strobe light, which measures the motor rpm.

The pedestal assembly, containing the propellant cup, buffer rod, and ultrasound transducer, is connected through the base of the combustion chamber by a threaded plug. This assembly is shown in Fig. 4. The ignition wiring is secured in a notch along the side of the pedestal and is insulated from contact with the pedestal.

More detail of the experimental setup can be found in Ref. 6. For steady-state experiments the rotating valve section is removed, and a one-nozzle throat section (Fig. 3b) replaces the two-nozzle throat configuration in Fig. 3a.

Data Acquisition and Reduction

A schematic of the ultrasound data-acquisition system as assembled by J. J. Murphy is shown in Fig. 5. The data-acquisition system digitally converts and records the analog signal displayed on the oscilloscope. Matlab® is then used in conjunction with various digital-signal-processing techniques to postprocess the data.

The transducer used in this study is a Panametrics V314, 1-MHz, spherically focused ultrasound transducer, with a focal length of 1.25 in. (31.75 mm). The active diameter is 0.75 in. (19.05 mm) with a -6 dB bandwidth of approximately 62% and a waveform duration of 2.1 μs at -14 dB.

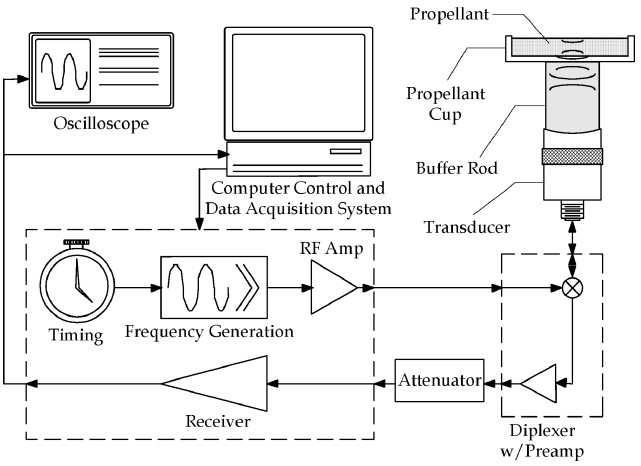

Fig. 5 Ultrasound data-acquisition system.

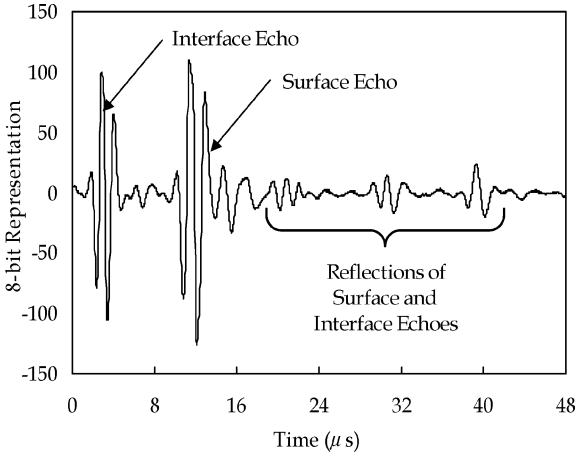

Fig. 6 8-bit digital representation of the analog ultrasound signal.

To ensure proper transmission of the ultrasound waves through the buffer rod, the bottom surface of the buffer rod must be machined to match the curvature of the focused transducer; the wear plate of the transducer has a radius of curvature of 0.90625 in. (23.02 mm). A thin layer of silicon gel is applied between the wear plate and buffer rod to ensure proper acoustic matching of the surfaces. A temperature-resistant couplant is applied between the propellant sample and the buffer rod, which serves to improve ultrasound transmission through the interface and protect the buffer rod from the high temperatures it would otherwise be exposed to at burnout.

The ultrasound transducer is pulsed by a Ritec RAM-10000 ultrasound system at a pulse repetition rate of up to 10 kHz. The pulse repetition rate utilized in this study is 2.5 kHz. The Ritec system also receives the echoes reflected from the burning surface of the propellant, which are subsequently recorded digitally at 25 MHz by a Gage Systems CS8500 high-speed data acquisition board.

Raw data taken from each test consist of a pressure trace taken from each of the two transducers and the digital representation of the analog ultrasound signal. The pressure and ultrasound data are synchronized in Matlab based upon a voltage output recorded by the Lab-VIEW® program that controls the system.

A schematic of a typical ultrasound waveform is shown in Fig. 6. The individual ultrasound waveforms are reconstructed by 1200 digitally converted (8-bit) points. Because the data are recorded at 25 MHz, the time interval between each of the 1200 points is 40 ns. A total of 2500 complete waveforms are sampled for every second of an experiment. Thus, each second of ultrasound data is stored in a 2500×1200 matrix.

The primary features of each waveform include echoes resulting from the buffer rod/propellant interface and the propellant's burning surface. The smaller echoes that are shown in Fig. 6 are secondary

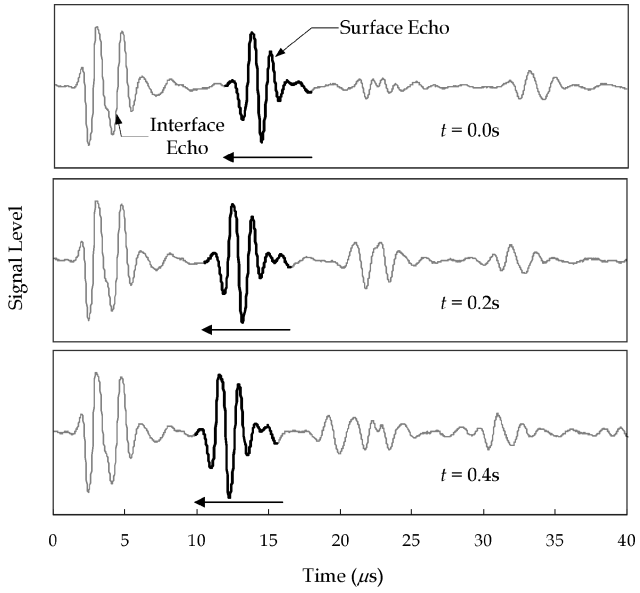

Fig. 7 Ultrasound echoes recorded 0.2 s apart during a 50 Hz experiment at 2.07 MPa.

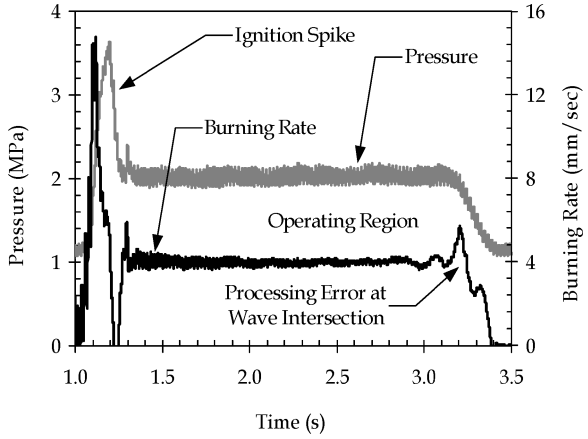

Fig. 8 Typical pressure and burning-rate curves from an oscillatory experiment.

reflections of the interface and burning surface. The translation of the surface echo toward the buffer rod during propellant combustion is shown in Fig. 7. It is the relative movement of this surface echo with respect to the interface echo that is the measurement of interest (i.e., the height/location of the solid-propellant burning surface).

A typical pressure trace for an experiment is shown in Fig. 8. The pressure trace is characterized by a region of prepressurization with helium gas that is followed by a short spike, which is produced by the rapid combustion of the ignition wafer. A region of constant mean pressure follows the ignition spike (operating region), which is indicative of a constant endburning surface area. It is within this region that data are taken for both response-function and burning-rate analysis. At burnout the pressure drops rapidly until the helium prepressurization level is reached.

Burning-Rate Calculation

Because burning rate is the time derivative of web thickness, the accuracy of the burning-rate calculation is entirely dependent upon the accuracy of the web thickness measurements, and therefore, a description of the web thickness calculation is provided next.

First, an estimate of the burning surface location is found by tracking the peak of the primary surface echo throughout a test. This estimate is then further refined by using a cross correlation, which is a tool typically utilized for time-delay estimation.[10] A Matlab subroutine is used to place a window of a known finite length around the primary features of the surface echo waveform. This window moves with the surface echo as it translates toward the buffer rod echo during an experiment. The cross correlation is performed upon two consecutive ultrasound frames. Thus at each finite time step the echo within the window is cross correlated with the same echo taken at the next sequential time step to obtain an accurate measure of the time delay between the two signals.

The expression for the cross correlation is given in Eq. (5):

$$\Re_{xy}(\tau) = \frac{1}{t_f}\int_0^{t_f} x(t)\,y(t+\tau)\,\mathrm{d}t \tag{5}$$

The actual time delay is taken as the value of τ at which the cross correlation attains its maximum.[11] To better resolve this maximum, a parabola is fit to the points in the neighborhood of the peak of the cross correlation. The actual time delay between the two signals is taken as the maximum of this parabolic fit; however, because a parabola only approximately represents these points, the fit results in a bias error of as much as $\pm\pi/\omega_0(\pm 0.5\ \mu\mathrm{s}$ using a 1-MHz transducer).[1]

The cross-correlation algorithm is demonstrated in Figs. 7 and 9. The calculation is performed on surface echoes shown in the first and second ($t = 0.0$ and 0.2 s) and first and third frames ($t = 0.0$ and 0.4 s) of Fig. 7, respectively. The results of these two calculations are shown in Fig. 9. A parabolic fit is applied to both cross correlations, and the maxima of the fits ($\tau_1 = 1.221\ \mu$s and $r_2 = 2.129\ \mu$s) are recorded as the time delay between the echoes.

The result of the time-delay analysis gives a time delay vs time profile for the test, which is converted to the original 1200-point representation of the ultrasound waveform by multiplying each time delay estimate by 25. This is possible because every 25 of the 1200 points utilized to reconstruct the ultrasound signal are actually representative of a 1-μs time delay. Thus, the time delays shown in Fig. 9 represent a movement of 30.525 and 53.225 points, respectively. The converted unscaled thickness profile is then scaled to the original height of the propellant h_0, which is measured prior to the experiment. This process is shown visually in Fig. 10.

Because of the dynamic nature of the experiment, a correction must be applied in the data analysis in order to account for several nonlinear transient effects. Specifically, movement of the buffer rod during a test resulting from pressure fluctuations, propellant combustion, and any vibrations associated with motor operation must be accounted for in the web thickness calculation. This is accomplished in much the same manner as the thickness calculation itself.

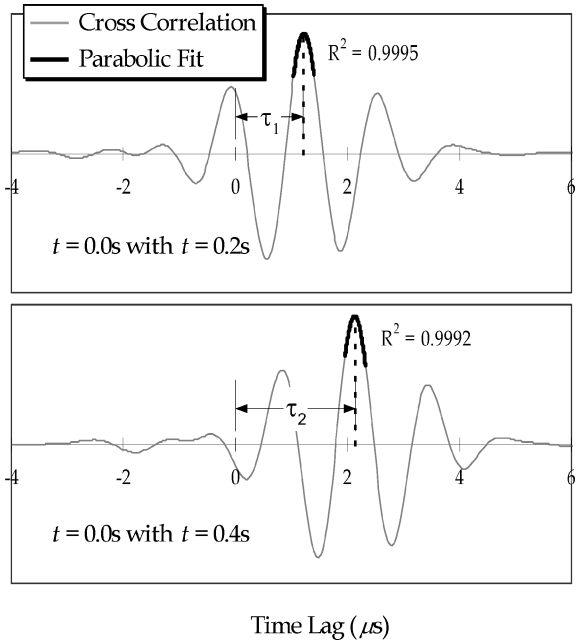

Fig. 9 Cross correlation and parabolic fit of the surface echoes shown in Fig. 7.

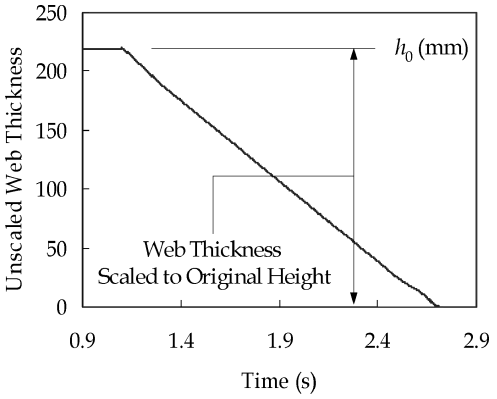

Fig. 10 Web thickness estimate for an experiment using Thiokol #10 at 100 Hz and 2.07 MPa.

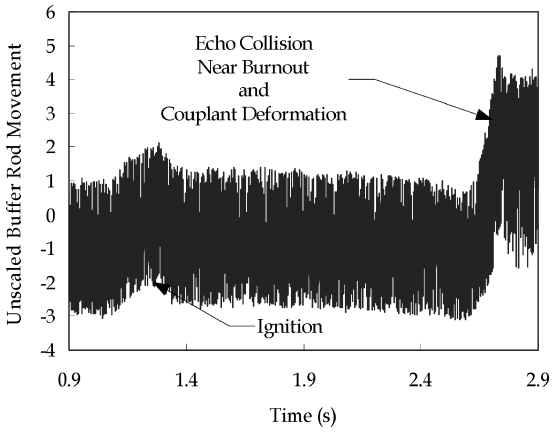

Fig. 11 Buffer rod correction for the experiment shown in Fig. 8.

A portion of the interface echo is tracked throughout a test by applying the cross correlation in Eq. (5) to the selected features of the interface. Thus, the time-delay history of the buffer rod is obtained, which is converted to the 1200-pt form similar to the web thickness calculation. The unscaled buffer rod correction is shown in Fig. 11. The buffer rod correction is subtracted from the unscaled thickness profile of the test. This result is then scaled to the original propellant height, thereby generating the final corrected web thickness of the experiment.

The second transient effect that must be accounted for in the thickness calculation concerns the interaction of the primary surface echo and the interface echo near burnout. When the surface echo collides with the interface, the two echoes interfere with one another. This phenomenon makes it difficult to resolve the movement of the surface echo at this point in time. Thus, it is necessary to separate the two waveforms to facilitate both tracking the peak and the cross-correlation algorithm. To this end, a reference interface waveform is subtracted out of each ultrasound frame. This process is depicted in Fig. 12. The reference waveform is selected prior to the point where any interference of the echoes occurs. This results in a surface waveform that most closely represents the actual location and shape of the true surface echo. However, because both the interface and surface echoes are moving with time some accuracy is lost when applying this correction, which is dependent upon the degree to which the echoes have collided.

Response-Function Calculation

The response function is calculated from the measured data through estimation of the spectral magnitude and phase of the burning rate and pressure signals at the frequency of the test. This is accomplished by taking the Fourier transform of the burning rate and dividing by the Fourier transform of the pressure, as shown in Eq. (3). An equivalent expression can be obtained in terms of web thickness.[2]

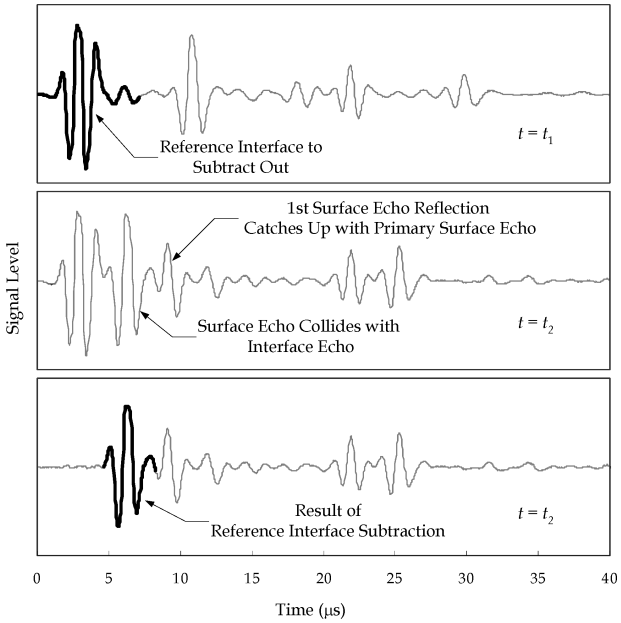

Fig. 12 Demonstration of the buffer rod reference interface subtraction.

$$R = i\omega(\bar{\dot{r}}/\bar{p})(G_x/G_p) \tag{6}$$

Equation (6) contains terms that are directly measured during each test.

The response calculation is further complicated because when the combustion chamber is pressurized the propellant is compressed. The compression results in a change in propellant thickness, as well as a change in the speed of sound within the sample. These fluctuations must be accounted for to acquire an accurate burning-rate measurement.

Pressure Correction

Once the combustion chamber has reached a steady mean pressure, it is a safe approximation to assume that viscoelastic effects can be ignored. Thus, for steady-state burning-rate measurements the pressure effects are corrected by an effective speed of sound c_{eff}, which accounts for both the compression of the propellant and fluctuations in the speed of sound. The effective speed of sound is obtained by pressurizing a chamber containing a nonburning propellant sample, while recording the change in round-trip time during the test, that is,

$$c_{\text{eff}}(p)/c_0 = \Delta t_0/\Delta t(p) \tag{7}$$

This value of c_{eff} can be used along with the round-trip time to calculate the web thickness for a steady-state experiment; however, this correction is not valid under transient pressure conditions. This is because experimental uncertainty in the measurement of the phase of the pressure and web thickness can introduce large errors into the pressure correction at high frequencies.[2] Therefore, the pressure correction for oscillatory tests must be treated separately.

The expression for the oscillatory pressure correction is obtained by first applying a perturbation to the derivative of Eq. (4). The response function then takes the following form[2]:

$$R_{\dot{r},p} \equiv \frac{\dot{r}'/\bar{\dot{r}}}{p'/\bar{p}} = i\omega \underbrace{\frac{\delta'/\bar{\delta}}{p'/\bar{p}}}_{\text{Measurement}} + \underbrace{\left(1 + i\omega\frac{\delta}{\bar{\dot{\delta}}}\right)\frac{\bar{p}}{\bar{c}_{\text{eff}}}\frac{\mathrm{d}c_{\text{eff}}}{\mathrm{d}p}}_{\text{Correction}} \tag{8}$$

which includes both a measurement and correction term. The second term of the correction factor dominates this equation for most of the duration of each experiment. This term includes the quantity δ, the round-trip time, which is approximately a linear function of web thickness. Therefore, a plot of the response as a function of

Table 1 Composition of MURI propellants available for testing

Designation	AP (%200/90/2–20μm)	AL, %	AN, %	Binder	Curative	Miscellaneous
Thiokol #4	53/0/33	——	——	HTPB	DDI	TMO (2%)
Thiokol #5	53/0/33	——	——	HTPB	IPDI	TMO (2%)
Thiokol #10	55/0/33	——	——	HTPB	DDI	——
Alliant #1	45/0/5	20	10	HTPE	——	——
Alliant #5	54/0/16	——	10	HTPE	——	——
Alliant #7	38/16/25	——	——	HTPE	——	——

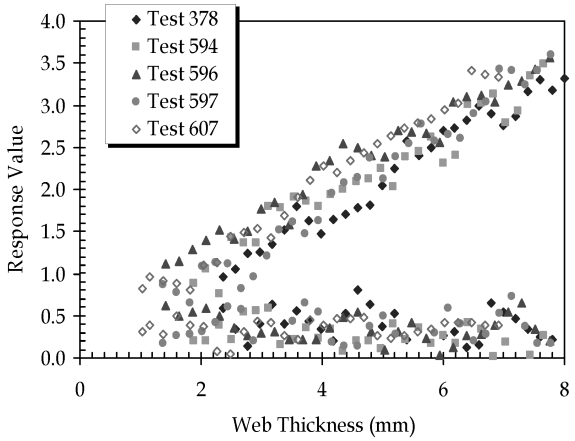

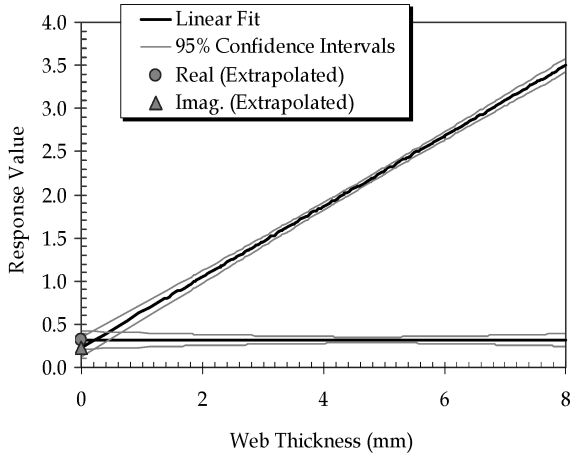

Fig. 13 Demonstration of the linear extrapolation for the real and imaginary parts of the response.

propellant height will exhibit a linear increase with web thickness. This can be seen visually in Fig. 13. Five tests performed at identical conditions ($f = 50$ Hz and $p = 2.07$ MPa) are shown in the plot. Clearly, both the real and imaginary parts of the response for all five tests are linearly dependent upon web thickness. The real and imaginary parts of the measured response function for all five tests are grouped together and fit to straight lines. This grouping is justified because samples of the same propellant should behave identically for the same test conditions. The linear fits are then extrapolated to zero web thickness (burnout) to obtain the response. This process is also shown in Fig. 13. Because the term proportional to web thickness is zero at burnout, the real and imaginary parts at this point represent the pressure corrected response for the test condition considered. In addition, because the fits are calculated from a group of observations, random error can be estimated from the statistics of those observations. The linear fits, therefore, not only provide estimated values of the real and imaginary parts of the response, but also 95% confidence intervals for those values.[11]

Results and Discussion

Compositions and labeling information for propellants supplied for testing are provided in Table 1. The propellants were provided by the Thiokol Propulsion Company, Alliant TechSystems, and United

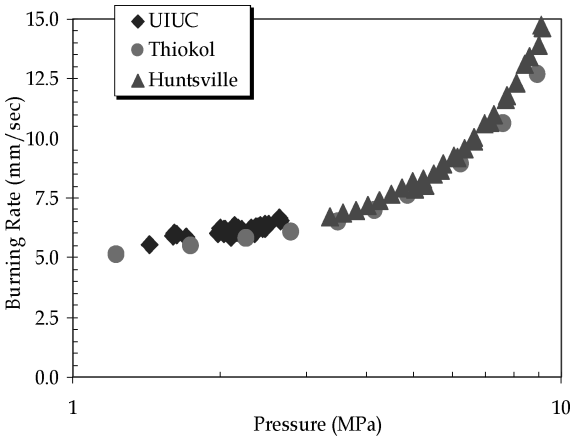

Fig. 14 Burning-rate data for Thiokol #4.

Technologies CSD as part of the Multi-Disciplinary University Research Initiative (MURI) program supported by the Ballistic Missile Defense Organization through the Office of Naval Research.[12] (Note that the Thiokol Propulsion Company has since merged with Alliant TechSystems. The propellant names are for identification purposes only.) Data are presented here for Thiokol #4, #5, #10 and Alliant #1, #5, and #7.

A summary of the test conditions and propellants utilized for burning-rate and response-function tests is given in the following two sections.

Burning-rate tests were performed for Thiokol #4, Thiokol #10, Alliant #5, and Alliant #7 over pressure ranges of 1–4 MPa (150–600 psi) in order to establish the accuracy of the ultrasound measurement system. Thiokol #5, a plateau propellant at high pressures, was chosen for a thorough burning-rate study for which steady-state and low-frequency oscillatory tests were performed at pressures between 2 and 14 MPa. This range contains a region of normal burning behavior that includes pressures from 2–10 MPa and a region of plateau behavior from 10–15 MPa. A particular emphasis was focused on the plateau region, where over 25 tests were performed. Oscillatory tests utilized frequencies ranging from 20–100 Hz for this study.

The response-function tests were performed with three primary objectives in mind. First, compositional effects on the response function were examined through comparison of data taken at pressures of 2.07 MPa (300 psi) and frequencies ranging from 20–200 Hz for two pairs of propellants. One propellant in each pair is a baseline propellant, and the second isolates one compositional variant. The second group of tests examined the effect of mean pressure on the response function. Thiokol #10 was selected for this study, and a series of tests were performed at two mean pressures (2.07 and 5.0 MPa—725 psi) at frequencies ranging from 20–200 Hz. The third and final response-function study investigated the response behavior within a plateau region. Thiokol #5 was selected for this study, and data were obtained at a mean pressure of 12.5 MPa and frequencies of 20 and 50 Hz.

Burning-Rate Results

Burning rates for Thiokol #4 and #10 are shown in Figs. 14 and 15, respectively. The burning rates obtained with the ultrasound method for Thiokol #4 are slightly higher than the steady-state values provided by the Thiokol Propulsion Company. However, similar

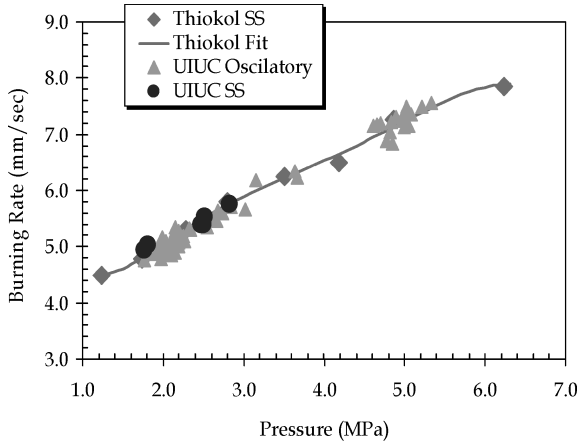

Fig. 15 Steady-state and oscillatory burning-rate data for Thiokol #10.

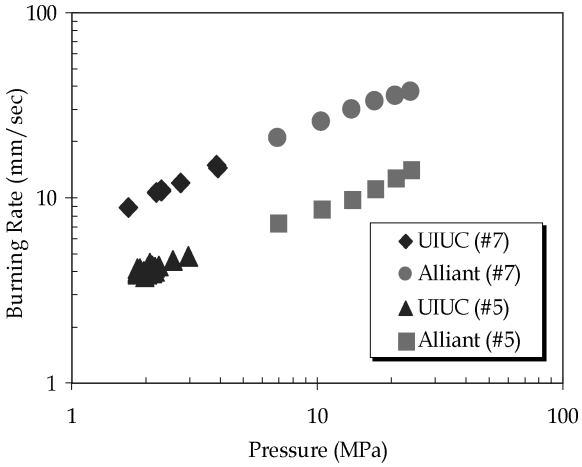

Fig. 16 Burning-rate data for Alliant #5 and Alliant #7.

behavior (greater burning rates) is evident when data taken with a closed bomb device at the University of Alabama at Huntsville[13] are compared with the steady-state Thiokol data. Very little scatter is evident in the ultrasound data, thereby demonstrating the precision of our technique. Clearly the data for Thiokol #10 show excellent agreement with steady-state data provided by Thiokol at all pressures tested. Again, there is very little scatter in the ultrasound burning rates.

Data for Alliant #5, a relatively slow burning propellant, and Alliant #7, a faster burning propellant, are shown in Fig. 16. Two compositional changes are responsible for the increased burning rate of Alliant #7. First, the coarse-to-fine oxidizer ratio is significantly reduced, and second, ammonium nitrate (10%) is not present in Alliant #7, which allows for a higher mass fraction of AP. This moves the composition closer to stoichiometric, increasing the adiabatic flame temperature. Although company data were not provided for the Alliant propellants at pressures below 6 MPa, the burning rates obtained with the ultrasound technique are consistent with the rate laws indicated by the high-pressure data.

Steady-state and oscillatory burning-rate results for Thiokol #5 (a plateau propellant) are given in Fig. 17. The ultrasound measurements are in excellent agreement below 12 MPa. Above 12 MPa, however, the ultrasound data show more scatter and generally higher burning rates than the Thiokol data. The higher burning rates and increased data scatter are corroborated by data obtained at the University of Alabama in Huntsville.[13] It appears the transient nature of the tests (10-mm samples burn out in less than 0.3 s at these pressures) combined with the dynamics of the plateau region results in the scatter seen in Fig. 17. Note that the ultrasound system is capable of obtaining accurate data for burning rates as high as 35 mm/s. This reinforces the assertion that the data scatter above 12 MPa is a result of the combustion dynamics within the plateau region.

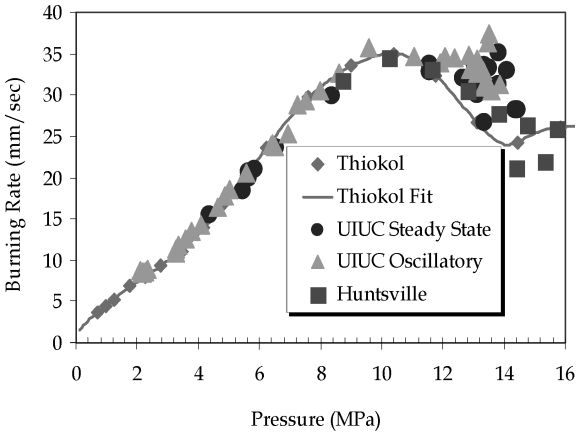

Fig. 17 Steady-state and oscillatory burning-rate data for Thiokol #5.

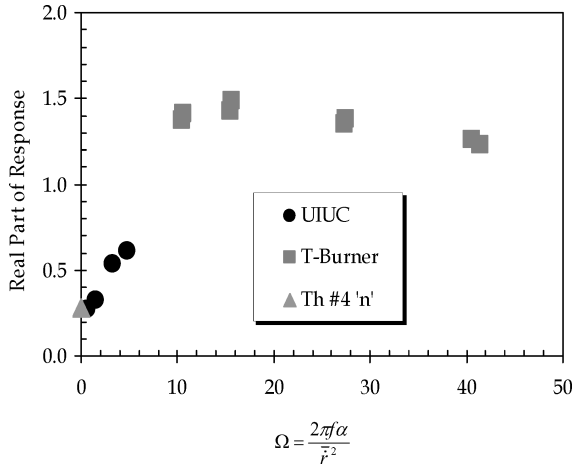

Fig. 18 Real part of the response of Thiokol #4: UIUC and T-Bruner data (2.07 MPa).

Response-Function Compositional Study

Two propellants manufactured by the Thiokol Propulsion Company were tested to determine the effect of a transition metal oxide (TMO) on the response function. Thiokol #4 was selected for comparison with the baseline propellant Thiokol #10. The lone difference between the propellants is the 2% addition of a TMO ballistic modifier to Thiokol #4. The coarse-to-fine ratios of AP are identical, as are the amounts of binder (HTPB) and curative dimeryl diisocyanate (DDI).

The second compositional study utilized two propellants manufactured by Alliant Techsystems to isolate the effect of aluminum addition on the response function. The propellant designated as Alliant #5 is the baseline propellant, containing only AP, hydroxy-terminated polyether (HTPE), and ammonium nirate (AN). Alliant #1 has a similar composition except that aluminum is added at 20%, which results in a 20% reduction of AP.

The response function data are plotted vs nondimensional frequency, $\Omega = 2\pi f \alpha / \bar{r}^2$. Values of $\alpha = 1.94 \times 10^{-3}$ cm^2/s and $\alpha = 2.58 \times 10^{-3}$ cm^2/s (Ref. 14) are used for nonaluminized and aluminized propellants, respectively. The tests were performed at actual frequencies ranging from 20–200 Hz.

The real part of the response for Thiokol #4 is plotted in Fig. 18. The data taken with the University of Illinois at Urbana–Champaign oscillatory burner technique are consistent with the trend suggested by the T-burner data taken at the Naval Air Warfare Center in China Lake.[15] Therefore, the data represent the low-frequency supplement to the T-burner data.

A critical characteristic of the data is that as frequency approaches zero the real part of the response approaches the steady-state value of the pressure exponent, that is, n.

A comparison of the response for the two Thiokol propellants is given in Fig. 19. The response of both propellants does approach

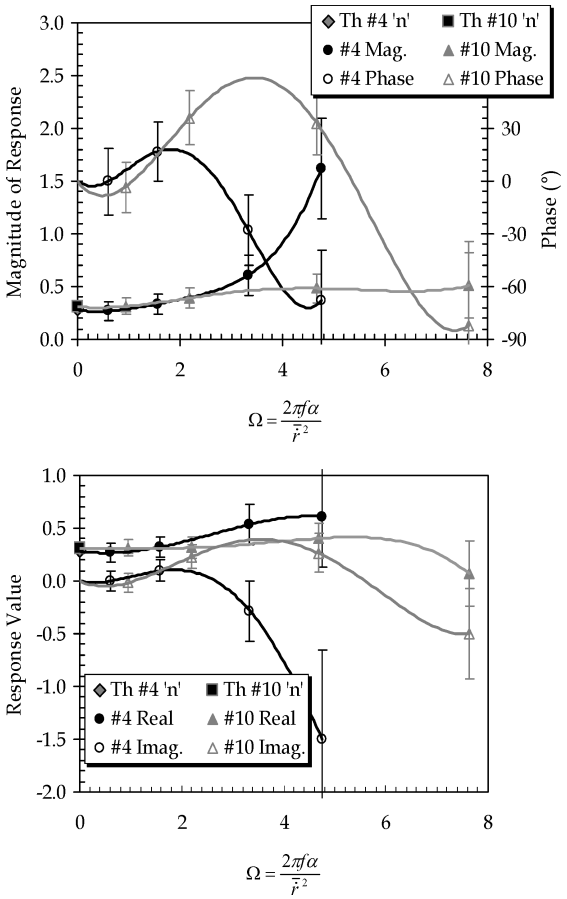

Fig. 19 Response-function data for Thiokol #4 and Thiokol #10 taken at 2.07 MPa.

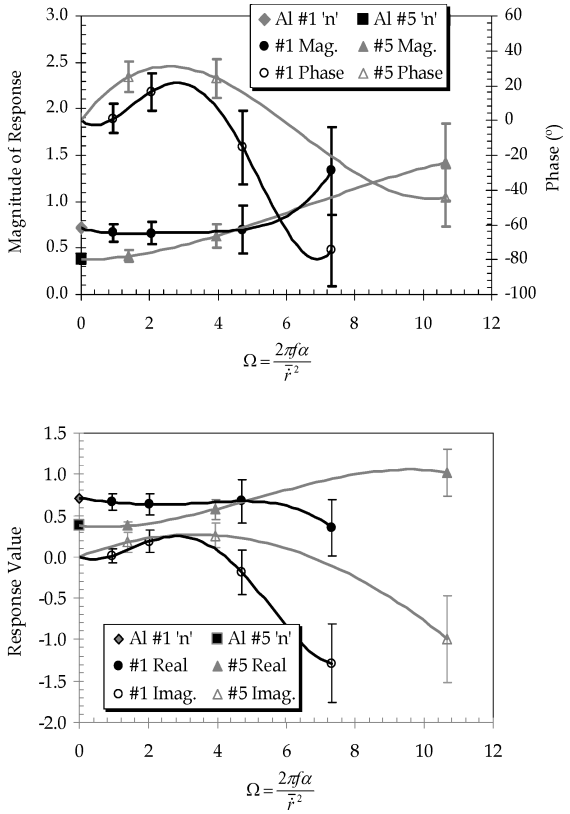

Fig. 20 Response-function data for Alliant #1 (aluminized) and Alliant #5 (unaluminized) taken at 2.07 MPa.

its respective value of n as frequency approaches zero. The real part of the response is the value of interest because the greater the real part of the response at a particular frequency, the greater the tendency is for the propellant to drive and couple with acoustic oscillations in the motor. From the phase data it is evident that, as expected, the burning rate at very low frequencies is in phase with the pressure for both propellants. Then the burning rate briefly leads the pressure as frequency increases and subsequently falls behind. The phase data are excellent indicators of the trend in the real part of the response. A propellant can only drive instabilities when the real part is positive and this can only occur when the phase lies between -90 deg and $+90$ deg. Near these upper- and lower-frequency limits the real part approaches zero and has no driving potential. This trend is evident with Thiokol #10. The real part of the response increases to a maximum at $\Omega \approx 5$ (100 Hz) and falls off to zero thereafter, which corresponds with the phase drop to near -90 deg. Although the phase of Thiokol #4 behaves similarly to Thiokol #10, Fig. 19 shows that the real part of the response for Thiokol #4 has yet to reach its maximum at $\Omega \approx 5$ (150 Hz). Therefore, the higher response for Thiokol #4 indicates it is less stable under the conditions tested than Thiokol #10. Thus, it can be stated that the TMO additive has an adverse effect on the stability of the propellant. The data for Thiokol #4 suggest that the TMO addition creates a greater increase in the burning rate when the propellant is subjected to a pressure transient at frequencies above $\Omega \approx 1.5$ (50 Hz), therefore indicating a better ability to drive instabilities. Indeed, it is evident from Fig. 19 that the magnitude for Thiokol #4 increases significantly more than Thiokol #10 with increasing frequency. This escalation dominates the phase lag and indicates that the magnitude of the burning-rate oscillations relative to the pressure oscillations for Thiokol #4 is growing with increasing frequency, which is undesirable behavior for motor stability.

Aluminum addition has long been known to have a stabilizing effect on propellant combustion under certain conditions. Although the primary stabilizing mechanism is particle damping in the rocket chamber, Fig. 20 shows that aluminum can also decrease the real part of the response function. The real part of the response for Alliant #1 (aluminized) does not reach a maximum peak, but rather attains its maximum at zero frequency and drops off thereafter. This is in contrast to Alliant #5 (nonaluminized), whose real part continuously increases with increasing frequency. The phase data further confirm this. The burning rate of Alliant #1 lags farther behind the pressure than Alliant #5 at each frequency. Data for Alliant #1 suggest that the addition of aluminum delays the response of the propellant to a pressure transient, effectively leaving the burning rate further out of phase with the pressure and unable to drive. Thus, the presence of aluminum in this propellant will promote rocket stability under these conditions.

Response-Function Mean Pressure Study

Results from experiments performed to evaluate the effect of mean pressure on the burning rate response for the Thiokol #10 propellant are shown in Fig. 21. The burning-rate response is plotted at two pressures: 2.0 and 5.0 MPa. Because the burning-rate parameters a and n in Eq. (1) are different at these two pressures (see Fig. 15), the real parts of the response at each mean pressure will approach dissimilar values at low frequency. Clearly, the mean pressure has a significant effect on the magnitude of the response function, which is evidenced by the increase in the magnitude at 5.0 MPa with increasing frequency. This discrepancy in the magnitude trends is accounted for by the significant decrease in the imaginary part of the response that accompanies the phase lag at the upper frequencies of the 5.0 MPa pressure condition. No distinguishing difference can be observed (within experimental uncertainty) in the real part of the response at the two mean pressures. Therefore, it can be concluded that the mean pressure has little effect on the stability of the propellant under these pressure and oscillatory frequency test conditions.

One of the principle processes controlling unsteady burning behavior in solid propellants is time lag of the thermal profile in the propellant. The quasi-steady homogeneous one-dimensional (QSHOD)

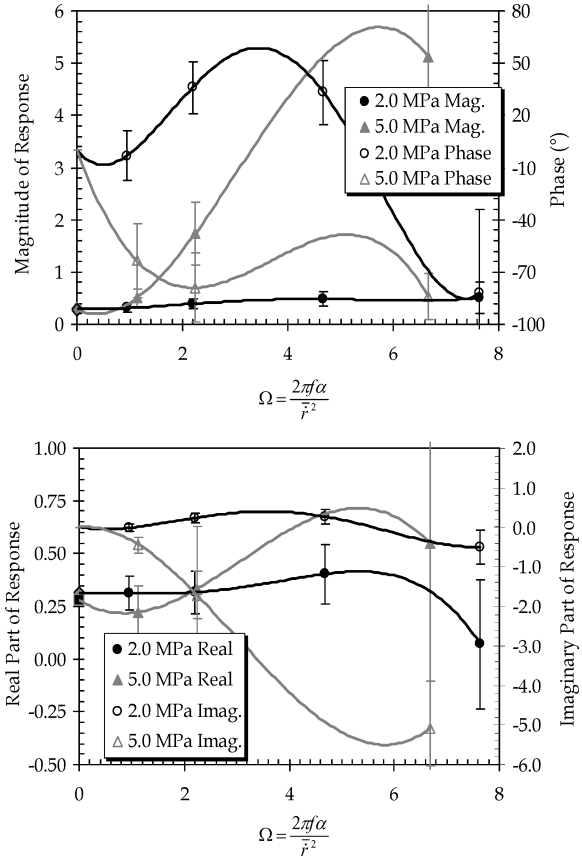

Fig. 21 Response-function data for Thiokol #10 taken at 2.0 and 5 .0 MPa.

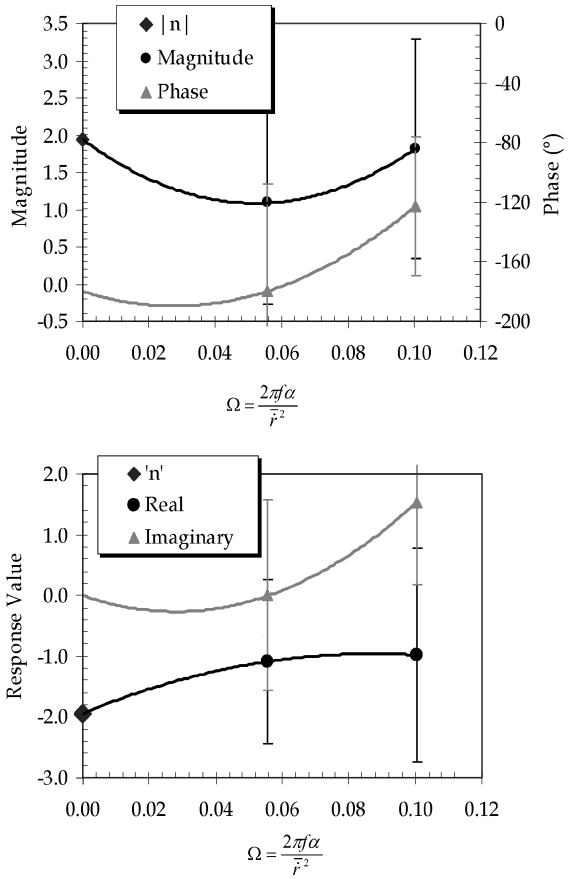

Fig. 22 Response-function data for Thiokol #5 taken within the plateau region (12.5 MPa).

family of response-function models describes this process. Although these models are strictly applicable to homogeneous propellants, they might be suitable for heterogeneous propellants as well for long timescales (low frequencies).[16] A tacit assumption made in most applications of QSHOD response models is the assumption of constant parameters (CP). If this assumption is correct, then response-function data taken at different pressures will collapse onto one curve when plotted as a function of the dimensionless frequency Ω. As stated in the preceding discussion, it is evident that the curves for the real part of the response do collapse; however, the curves for the imaginary part clearly do not, indicating that the CP assumption does not hold for the imaginary part of the response function.

Response-Function Plateau Study

The results just shown demonstrate that the real part of the response function for a composite propellant approaches the value of the pressure exponent n in the burning-rate law as frequency approaches zero. This is an important observation for stability prediction of solid-rocket motors. Burning-rate data for Thiokol #5, a plateau propellant, were shown in Fig. 17. Note that in the region between 10 and 14 MPa the burning-rate curve in Fig. 17 has a negative slope, which is indicative of a negative pressure exponent. The implications of this phenomenon are significant because the real part of the response function must approach this negative value as frequency approaches zero, and the burning rate will therefore be 180 deg out of phase with the pressure. Thus, the propellant will have no potential to drive instability at low frequencies.

A study was performed within the plateau region for Thiokol #5 to verify this theorized negative behavior of the real part of the response. The results of this study are shown in Fig. 22. Clearly the real part of the response does approach the value of the pressure exponent at low frequency. This negative behavior indicates that the propellant is stable at these frequencies (50 and 100 Hz) within the plateau and has no ability to drive instabilities. From the phase data in Fig. 22, it is clear that the burning rate is 180 deg out of phase with the pressure oscillations, leaving it unable to couple with the pressure and drive. The decreasing magnitude supports this stability assertion, because the magnitude is seen to decrease with increasing frequency. Thus, it can be concluded that motors operating at pressures within a plateau region will be stable at low frequency and likely even at higher-frequency conditions.

Conclusions

Through both steady-state tests and response-function measurements, the ultrasound method presented here allows for accurate burning-rate measurements under a variety of oscillatory pressure conditions. In addition, changes in propellant composition were shown to create significant differences in the response. Aluminum produced a stabilizing effect on the response by delaying the propellant's reaction to pressure transients in such a way that the burning rate lies out of phase with the pressure and is unable to drive. Also, the TMO additive was shown to increase a propellant's driving potential by amplifying the burning-rate oscillations with respect to pressure as frequency increases. Finally, response function data taken at a mean pressure within the plateau region of a composite propellant showed that motors are stable at low frequency when operating within a plateau region.

Data presented here not only offer valuable information about the effect of additives and pressure on the pressure-coupled response of composite propellants, but also demonstrate the ability of ultrasound to extend past the steady-state realm to make thickness measurements under transient pressure conditions. Although the data presented have an upper-frequency range of 200 Hz, this does not indicate that ultrasound cannot be utilized beyond this limit. Even though the uncertainty for response data increases with frequency, this is most likely a result of the corresponding decrease in the amplitude of the pressure oscillations as well as the sampling rate and waveform reconstruction. Changing the chamber volume, increasing the sampling rate, and reconstructing the ultrasound signal with more points per waveform can undoubtedly improve measurement accuracy.

Acknowledgments

This work was funded through The Center for the Simulation of Advanced Rockets (CSAR) at University of Illinois at Urbana–Champaign, Michael Heath, director. The CSAR research program is supported by the U.S. Department of Energy through the University of California under subcontract B341494. Additional funding provided by the Ballistic Missile Defense Organization through the Office of Naval Research Contract N00014-95-1-1339 as part of the University of Illinois at Urbana—Champaign Multi-Disciplinary University Research Initiative Center for the Study of Novel Energetic Materials. The authors would also like to thank William D. O'Brien for his assistance with the development and implementation of the ultrasound data-acquisition system. In addition, the work presented here would not have been possible without the efforts in the laboratory by the following undergraduate students: Patricia Cannon, Justin Roy, Erik Solverson, and Nathan Bergland.

References

[1]Murphy, J. J., and Krier, H., "Ultrasound Measurements of Transient Burning Rates of Solid Propellants," *Journal of Propulsion and Power*, Vol. 18, No. 3, 2002, pp. 641–651.

[2]Murphy, J. J., "Measurement and Modeling of Pressure-Driven Transient Burning of Solid Propellants," Ph.D. Dissertation, Dept. of Mechanical and Industrial Engineering, Univ. of Illinois at Urbana-Champaign, Urbana, 2000.

[3]Coates, R. L., Horton, M. D., and Ryan, N. W., "T-Burner Method of Determining the Acoustic Admittance of Burning Propellants," *AIAA Journal*, Vol. 2, No. 6, 1964, pp. 1119–1122.

[4]Horton, M. D., "Use of the One-Dimensional T-Burner to Study Oscillatory Combustion," *AIAA Journal*, Vol. 2, No. 6, 1964, pp. 1112–1118.

[5]Korting, P .A. O. G., and Schöyer, H. F. R., "Determination of the Regression Rate in Solid Fuel Ramjets by Means of the Ultrasonic Pulse Echo Method," *Heat Transfer in Fire and Combustion Systems*, ASME HTD 45, 1985, pp. 347–353.

[6]Fuchinoue, R., "Development of the Oscillatory Burner to Measure the Pressure-Coupled Response Function," M.S. Thesis, Dept. of Mechanical and Industrial Engineering, Univ. of Illinois at Urbana—Champaign, Urbana, 1999.

[7]Brdar, C. R., "Ultrasonic Echo-Location for Solid Propellant Response Function Measurement," M.S. Thesis, Dept. of Mechanical and Industrial Engineering, Univ. of Illinois at Urbana—Champaign, Urbana, 2001.

[8]Chai, S., "Pressure-Coupled Response Function Measurement using an Ultrasound Echo-Location Technique," M.S. Thesis, Dept. of Mechanical and Industrial Engineering, Univ. of Illinois at Urbana—Champaign, Urbana, 2000.

[9]Brown, R. S., "Development and Evaluation of a Rotating Valve Combustion Response Test Technique," Chemical Systems Div./United Technologies, AFRPL-TR-76-72, 1976.

[10]Carter, G. C., "Time Delay Estimation," *IEEE Transactions on Acoustics, Speech, and Signal Processing*, Vol. ASSP-29, No. 3, 1981, p. 461.

[11]Bendat, J. S., and Persol, A. G., *Random Data Analysis and Measurement Procedures*, 2nd ed., Wiley, New York, 1986.

[12]Office of Naval Research, Contract N-0014-95-1-1339.

[13]Chiyyarath, K., "Ballistic Characteristics of Bi-Plateau Solid Propellants," M.S. Thesis, Univ. of Alabama in Huntsville, 1998.

[14]Zanotti, C., Volpi, A., Bianchessi, M., and Luca, L. D., "Measuring Thermodynamic Properties of Burning Propellants," *Nonsteady Burning and Combustion Stability of Solid Propellants*, edited by L. D. Luca, E. W. Price, and M. Summerfield, AIAA, Washington, D.C., 1992, pp. 145–196.

[15]Blomshield, F. S., and Stalnaker, R. A., "Combustion Response of Bi-Plateau Propellants," 34th JANNAF Combustion Subcommittee Meeting, West Palm Beach, Florida, CPIA 662, Oct. 1997, pp. 169–178.

[16]Murphy, J. J., and Krier, H., "Linear Pressure Coupled Frequency Response of Heterogeneous Solid Propellants," *Proceedings of the 27th Symposium (International) on Combustion*, The Combustion Inst., 1998.